Human oxygen sensing may have origins in prokaryotic elongation factor Tu prolyl-hydroxylation

John S. Scotti[a], Ivanhoe K. H. Leung[a,1,2], Wei Ge[a,b,1], Michael A. Bentley[c], Jordi Paps[d], Holger B. Kramer[e], Joongoo Lee[a], WeiShen Aik[a], Hwanho Choi[a], Steinar M. Paulsen[c,3], Lesley A. H. Bowman[f], Nikita D. Loik[a,4], Shoichiro Horita[a,e], Chia-hua Ho[a,5], Nadia J. Kershaw[a,6], Christoph M. Tang[f], Timothy D. W. Claridge[a], Gail M. Preston[c], Michael A. McDonough[a], and Christopher J. Schofield[a,7]

[a]Chemistry Research Laboratory, Department of Chemistry, University of Oxford, Oxford OX1 3TA, United Kingdom; [b]Chinese Academy of Medical Sciences, Beijing 100005, China; [c]Department of Plant Sciences, University of Oxford, Oxford OX1 3RB, United Kingdom; [d]Department of Zoology, University of Oxford, Oxford OX1 3PS, United Kingdom; [e]Department of Physiology, Anatomy, and Genetics, University of Oxford, Oxford OX1 3QX, United Kingdom; and [f]Department of Pathology, University of Oxford, Oxford OX1 3RE, United Kingdom

Edited by Gregg L. Semenza, The Johns Hopkins University School of Medicine, Baltimore, MD, and approved August 5, 2014 (received for review May 30, 2014)

The roles of 2-oxoglutarate (2OG)-dependent prolyl-hydroxylases in eukaryotes include collagen stabilization, hypoxia sensing, and translational regulation. The hypoxia-inducible factor (HIF) sensing system is conserved in animals, but not in other organisms. However, bioinformatics imply that 2OG-dependent prolyl-hydroxylases (PHDs) homologous to those acting as sensing components for the HIF system in animals occur in prokaryotes. We report cellular, biochemical, and crystallographic analyses revealing that *Pseudomonas* prolyl-hydroxylase domain containing protein (PPHD) contain a 2OG oxygenase related in structure and function to the animal PHDs. A *Pseudomonas aeruginosa PPHD* knockout mutant displays impaired growth in the presence of iron chelators and increased production of the virulence factor pyocyanin. We identify elongation factor Tu (EF-Tu) as a PPHD substrate, which undergoes prolyl-4-hydroxylation on its switch I loop. A crystal structure of PPHD reveals striking similarity to human PHD2 and a *Chlamydomonas reinhardtii* prolyl-4-hydroxylase. A crystal structure of PPHD complexed with intact EF-Tu reveals that major conformational changes occur in both PPHD and EF-Tu, including a >20-Å movement of the EF-Tu switch I loop. Comparison of the PPHD structures with those of HIF and collagen PHDs reveals conservation in substrate recognition despite diverse biological roles and origins. The observed changes will be useful in designing new types of 2OG oxygenase inhibitors based on various conformational states, rather than active site iron chelators, which make up most reported 2OG oxygenase inhibitors. Structurally informed phylogenetic analyses suggest that the role of prolyl-hydroxylation in human hypoxia sensing has ancient origins.

The hypoxia-inducible transcription factor (HIF) is a major regulator of the response to limited oxygen availability in humans and other animals (1–3). A hypoxia-sensing component of the HIF system is provided by 2-oxoglutarate (2OG)-dependent and Fe(II)-dependent oxygenases, which catalyze prolyl-4-hydroxylation of HIF-α subunits, a posttranslational modification that enhances binding of HIF-α to the von Hippel-Lindau protein (pVHL), so targeting HIF-α for proteasomal degradation. The HIF prolyl-hydroxylases (PHDs) belong to a subfamily of 2OG oxygenases that catalyze prolyl-hydroxylation, which also includes the collagen prolyl-3-hydroxylases (CP3Hs) and prolyl-4-hydroxylases (CP4Hs) (4). Subsequently identified prolyl-hydroxylases include the ribosomal prolyl-hydroxylases (OGFOD1 and Tpa1), which catalyze ribosomal protein 23 prolyl-3-hydroxylation in many eukaryotes, and slime-mold enzymes, which catalyze prolyl-4-hydroxylation of Skp1, a ubiquitin ligase subunit (5–9). The HIF-PHD-VHL triad is likely present in all animals, but probably not in other organisms (3). However, structurally informed bioinformatic analyses imply the presence of PHD homologs in bacteria (10, 11), including in *Pseudomonas spp*, suggesting PHDs may have ancient origins.

Results

***Pseudomonas spp.* Contain a Functional PHD.** To investigate the role of a putative PHD homolog in *Pseudomonas aeruginosa* (PPHD), we initially characterized a *PPHD* insertional mutant strain. Metabolic screening studies revealed that the *PPHD* mutant strain displays impaired growth in the presence of iron chelators (e.g., 2,2-bipyridine) and produces increased levels of the bacterial virulence factor pyocyanin (*SI Appendix*, Fig. S1) (12), implying PPHD is involved in iron regulation. Ferrous iron is essential for PHD catalysis and treatment of human cells with iron chelators,

Significance

The Fe(II)- and 2-oxoglutarate (2OG)-dependent hypoxia-inducible transcription factor prolyl-hydroxylases play a central role in human oxygen sensing and are related to other prolyl-hydroxylases involved in eukaryotic collagen biosynthesis and ribosomal modification. The finding that a PHD-related prolyl-hydroxylase in *Pseudomonas spp.* regulates pyocyanin biosynthesis supports prokaryotic origins for the eukaryotic prolyl-hydroxylases. The identification of the switch I loop of elongation factor Tu (EF-Tu) as a *Pseudomonas* prolyl-hydroxylase domain containing protein (PPHD) substrate provides evidence of roles for 2OG oxygenases in both translational and transcriptional regulation. A structure of the PPHD:EF-Tu complex, the first to the authors' knowledge of a 2OG oxygenase with its intact protein substrate, reveals that major conformational changes occur in both PPHD and EF-Tu and will be useful in the design of new prolyl-hydroxylase inhibitors.

Author contributions: J.S.S., I.K.H.L., W.G., G.M.P., M.A.M., and C.J.S. designed research; J.S.S., I.K.H.L., W.G., M.A.B., J.P., H.B.K., J.L., W.A., H.C., S.M.P., L.A.H.B., N.D.L., C.-h.H., and N.J.K. performed research; J.S.S. contributed new reagents/analytic tools; J.S.S., I.K.H.L., W.G., M.A.B., J.P., H.B.K., C.M.T., T.D.W.C., G.M.P., M.A.M., and C.J.S. analyzed data; and J.S.S., S.H., M.A.M., and C.J.S. wrote the paper.

The authors declare no conflict of interest.

Data deposition: The atomic coordinates have been deposited in the Protein Data Bank, www.pdb.org (PDB ID codes 4J25, 4J0Q, 4IW3), and sequence data deposited in Uniprot, www.uniprot.org/uniprot (accession nos. Q88CM1 and Q9I6I1) and GenBank, www.ncbi.nih.gov/protein (accession nos. AAN70724.1 and AAG03699.1).

[1]I.K.H.L. and W.G. contributed equally to this work.

[2]Present address: School of Chemical Sciences, University of Auckland, Auckland 1142, New Zealand.

[3]Present address: Department of Medical Biology, University of Tromsø, N-9019 Tromsø, Norway.

[4]Present address: Department of Chemistry, University of Tokyo, 113-0033 Tokyo, Japan.

[5]Present address: Helmholtz Zentrum Munchen, 85765 Munchen, Germany.

[6]Present address: The Walter and Eliza Hall Institute of Medical Research, Parkville, VIC 3052, Australia.

[7]To whom correspondence should be addressed. Email: christopher.schofield@chem.ox.ac.uk.

This article contains supporting information online at www.pnas.org/lookup/suppl/doi:10.1073/pnas.1409916111/-/DCSupplemental.

including pyocyanin (13), and causes HIF-α up-regulation via PHD inhibition, suggesting related roles for PPHD and the animal PHDs (1).

Elongation Factor Tu Is a PPHD Substrate. We then investigated possible PPHD substrates. Mass spectrometric (MS) studies identified elongation factor Tu (EF-Tu) as a PPHD binding partner and potential substrate in *Pseudomonas putida* (*SI Appendix*, Table S3). This assignment is supported by a proteomic MS study on *Shewanella oneidensis*, reporting that EF-Tu is modified by a +16-Da mass shift (14); bioinformatics reveal *Shewanella oneidensis* contains a potential hydroxylase closely related to PPHD (38% identity). We tested a set of 14 synthetic peptides covering the 19 prolines in the EF-Tu sequence as substrates for isolated recombinant $PPHD_{putida}$ (*SI Appendix*, Table S4). We identified an EF-Tu peptide as undergoing a +16-Da mass shift (Fig. 1*B* and *SI Appendix*, Table S4); MSMS analyses demonstrated hydroxylation at Pro54 (Hyp54; *SI Appendix*, Fig. S2*A*). Amino acid analyses reveal that $PPHD_{putida}$ catalyzes *trans* prolyl-4-hydroxylation of EF-Tu, as occurs for PHD-catalyzed HIF and CP4H-catalyzed collagen prolyl-hydroxylation (*SI Appendix*, Fig. S2*B*) (1). We did not observe cross hydroxylation reactivity between the PPHD and PHD2 substrates; that is, EF-Tu with PHD2 and the *C*-terminal oxygen degradation domain (CODD) of HIF-1α ($CODD_{556–574}$) with PPHD.

EF-Tu undergoes hydroxylation in the wild-type but not in the *PPHD* insertional mutant strain, as shown by MS studies (*SI Appendix*, Fig. S3*A* and *B*). Because the human elongation factor 2 (eEF2) interacts with PHD2 (15), we tested peptides derived from the switch I loop of human eEF2 as potential PPHD or PHD2 substrates but did not observe hydroxylation within the limits of detection.

Effect of Prolyl-Hydroxylation on EF-Tu Function. Kinetic analyses were then carried out using a 20-residue EF-Tu fragment ($EF\text{-}Tu_{44–63}$). Compared with an analogous substrate fragment with PHD2, $PPHD_{putida}$ has a similar apparent K_m (47.2 ± 8.5 μM for PPHD/$EF\text{-}Tu_{44–63}$; 36.7 ± 9.0 μM for PHD2/HIF-1α CODD), but a lower apparent K_m for O_2 (47.5 ± 9.2 μM for PPHD/$EF\text{-}Tu_{44–63}$; 229 ± 60 μM for PHD2/HIF-1α CODD), and higher apparent K_m values for 2OG (182 ± 22 μM for PPHD/$EF\text{-}Tu_{44–63}$; 55 ± 11 μM for PHD2/HIF-1α CODD), Fe(II) (6.3 ± 0.7 μM for PPHD/$EF\text{-}Tu_{44–63}$; <1 μM for PHD2/HIF-1α CODD), and L-ascorbate (1,064 ± 95 μM for PPHD/$EF\text{-}Tu_{44–63}$; 54 ± 10 μM for PHD2/HIF-1α CODD; *SI Appendix*, Fig. S4 *A–E*) (16–20). Although the results with isolated enzyme may not reflect the cellular kinetics, given that PHD2 kinetics are proposed to reflect its role as a hypoxia sensor, these preliminary differences are of interest. In particular, the higher K_m for Fe(II) is notable given the phenotypic results on the *PPHD* insertional mutant strain, supporting a role for PPHD in iron regulation.

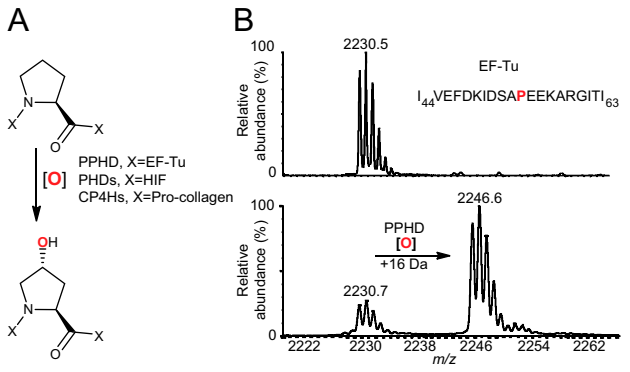

Fig. 1. Identification of EF-Tu as a $PPHD_{putida}$ substrate. (*A*) $PPHD_{putida}$, human HIF (PHDs), and collagen (CP4Hs) prolyl-4-hydroxylases catalyze 4-*trans* prolyl-hydroxylation. (*B*) EF-Tu is a $PPHD_{putida}$ substrate; MS spectrum showing a +16-Da peak revealing $PPHD_{putida}$-dependent prolyl-4-hydroxylation of $EF\text{-}Tu_{44–63}$.

The switch I loop of EF-Tu plays a central role in bacterial translation by coupling GTP hydrolysis with conformational changes from the GTP-bound active state to the GDP-bound inactive state (21, 22). NMR was used to directly monitor kirromycin-induced GTP hydrolysis by $EF\text{-}Tu_{putida}$; we observed no difference in the GTP hydrolysis rate for Hyp54 EF-Tu (0.71 ± 0.02 μM/min) and unmodified EF-Tu (0.76 ± 0.08 μM/min; *SI Appendix*, Fig. S5*A*). However, addition of $PPHD_{putida}$ to the EF–Tu GTP hydrolysis reaction decreased the rate of GTP hydrolysis in a metal ion and 2OG-dependent manner [Zn(II) 0.60 ± 0.05 μM/min; Zn(II) and 2OG 0.49 ± 0.16 μM/min; Zn(II) was used as a surrogate for Fe(II) and a $PPHD_{putida}$ inhibitor; *SI Appendix*, Fig. S5 *B–D*]. In *P. aeruginosa*, we observed no difference in the global translation rate between the *PPHD* mutant strain and the wild-type under standard growth conditions, as measured by [^{35}S]methionine incorporation (*SI Appendix*, Fig. S5*E*). The effect of $PPHD_{putida}$ on the GTP hydrolysis rate is less with hydroxylated EF-Tu (0.83 ± 0.08 μM/min) (*SI Appendix*, Fig. S5*B*), likely because of the weaker binding of hydroxylated EF-Tu to PPHD.

Using a paramagnetic relaxation enhancement-based NMR technique [with Mn(II) substituting for Fe(II)], we observed that addition of $EF\text{-}Tu_{protein}$ decreased the $PPHD_{putida}$ 2OG K_d by ~50-fold (8 ± 4 μM) compared with the absence of any substrate or in the presence of $EF\text{-}Tu_{44–63}$ (>400 μM; *SI Appendix*, Fig. S5*F*), implying a substantial interaction interface between $PPHD_{putida}$ and EF-Tu. These results implied that very substantial interactions between $PPHD_{putida}$ and EF-Tu likely extend well beyond the immediate active site region. Notably, the observation that $PPHD_{putida}$ addition decreases the rate of GTP hydrolysis and the location of Pro54 on the switch I loop suggests that $PPHD_{putida}$ sequesters the switch I loop. We therefore pursued structural characterization of $PPHD_{putida}$, EF-Tu, and the PPHD:EF-Tu complex.

Structure of PPHD. To investigate the structural similarity of $PPHD_{putida}$ to PHD2, we determined a crystal structure of $PPHD_{putida}$ complexed with Mn(II) and *N*-oxalylglycine (NOG), which are inert substitutes for Fe(II) and 2OG, respectively (2.0-Å resolution; space group *P*1). Similar to other 2OG oxygenases, $PPHD_{putida}$ contains a double-stranded β-helix (DSBH) core fold comprising eight β-strands (I–VIII) folded into major and minor β-sheets that enclose the metal-/2OG-binding sites (Fig. 2*A*) (23, 24). Five antiparallel β-strands [β1-β2(I)-β4(III)-β7(VI)-β9(VIII)] form the major β-sheet, and four antiparallel β-strands [β3(II)-β5(IV)-β6(V)-β8(VII)] form the minor β-sheet. Three α-helices (α1–α3) pack against the major β-sheet of the DSBH. A disordered region (residues 47–71) of $PPHD_{putida}$ corresponds to the β2–β3 finger loop of PHD2, which is conformationally flexible and involved in HIF-α binding (10, 25). $PPHD_{putida}$ contains a HXD...H triad of metal-binding residues (His124, Asp126, and His183), which, with the NOG oxalyl group and a water, complete octahedral metal-coordination. Although nonidentical, the $PPHD_{putida}$ active site is very similar to that of PHD2 (10); NOG is positioned between the major and minor β-sheets of the DSBH such that its C-5 carboxylate forms a salt bridge with Arg192 ($Arg383_{PHD2}$) (Fig. 2 *B* and *C*). The clear similarity between $PPHD_{putida}$ and PHD2 supports the proposal of common ancestry for the two hydroxylases (Fig. 2*B*).

Structure of a PPHD:EF-Tu Complex. We determined a *P. putida* EF-Tu structure (2.3-Å resolution; space group *C*2). $EF\text{-}Tu_{putida}$ and *Escherichia coli* EF-Tu have very similar overall folds (rmsd, 1.5 Å over 353 Cα atoms) and Mg(II) binding sites in their inactive GDP-bound states (Fig. 3*A* and *SI Appendix*, Fig. S6 *A* and *B*) (26). The switch I loop of $EF\text{-}Tu_{putida}$ (residues 40–62) is disordered; this is notable because the prolyl-hydroxylated regions of HIF-α are also predicted to be disordered in solution (18).

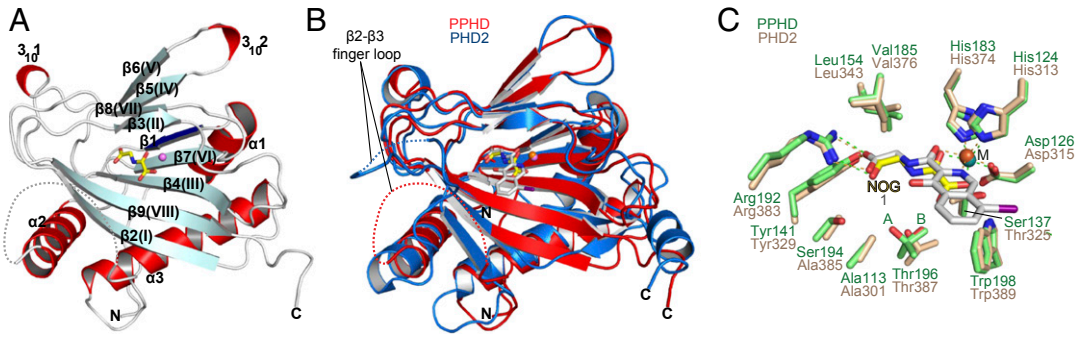

Fig. 2. PPHD$_{putida}$ is structurally similar to human PHD2. (*A*) Ribbons representation of the overall structure of PPHD$_{putida}$; DSBH-associated β-strands (pale cyan), roman numerals indicate strands in the DSBH, DSBH-extension β-strands (dark blue), α-helices (red), loops (white), NOG (yellow), Mn(II) (pink sphere). (*B*) Superposition of the PPHD$_{putida}$(red):NOG (yellow) and human PHD2 (blue):1 (gray) (PDB ID: 2G1M; rmsd, 1.7 Å over 181 Cα atoms) structures. (*C*) Superimposition of active site residues of PPHD$_{putida}$ (green):NOG (yellow) and human PHD2 (light-brown):1 (gray) (PDB ID: 2G1M) [1: *N*-(4-hydroxy-8-iodoisoquinolin-3-yl)carbonylglycine].

To obtain a structure of a PPHD:EF-Tu protein–protein complex (Fig. 3 *A*–*C*), PPHD and EF-Tu were expressed separately to prevent EF-Tu hydroxylation and then mixed, purified, and crystallized using Mn(II) and NOG to stabilize and inactivate/inhibit PPHD, and Mg(II) and GDP to stabilize EF-Tu. In the resultant PPHD:EF-Tu complex structure (2.7-Å resolution; $P3_1\,2\,1$),

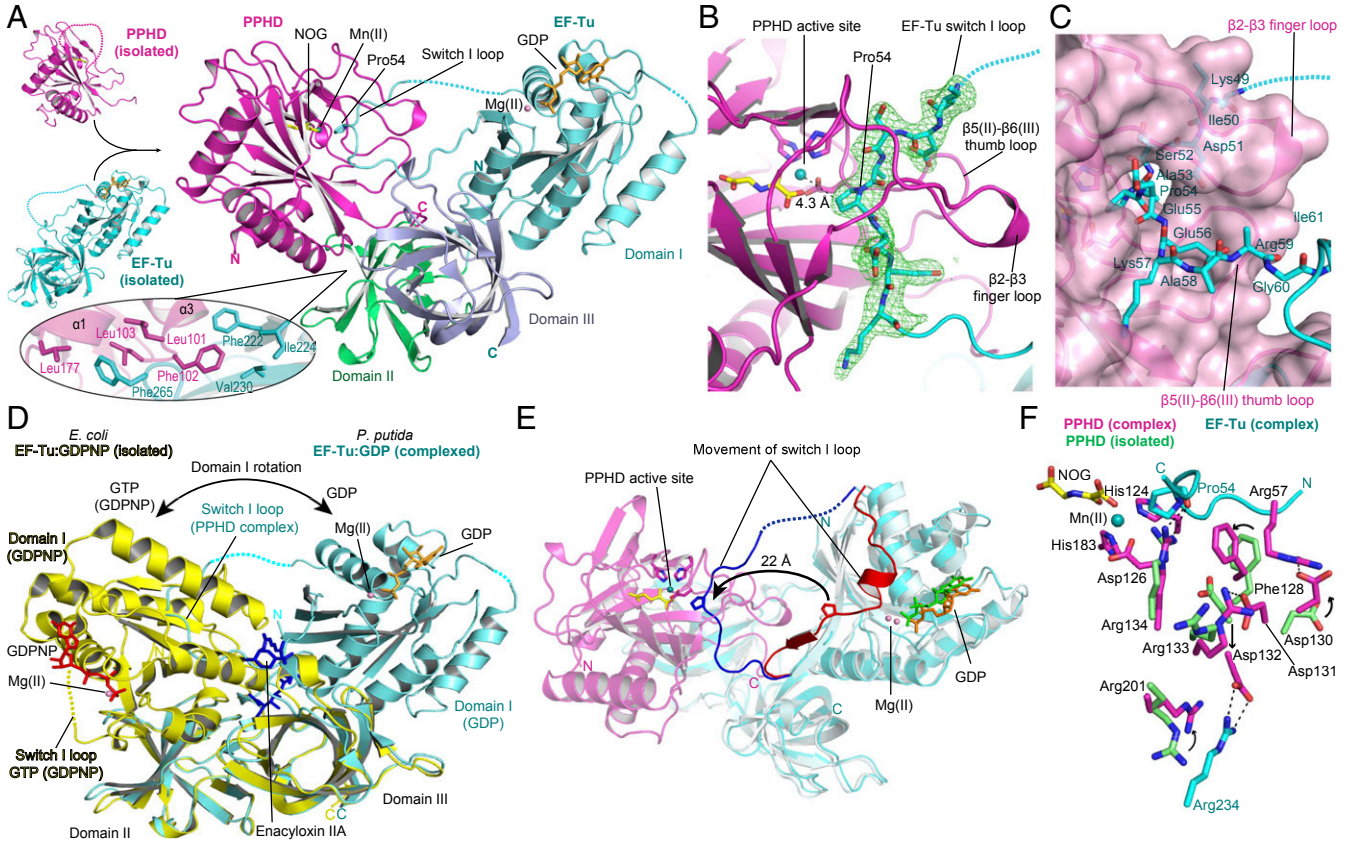

Fig. 3. A PPHD:EF-Tu complex structure reveals major conformational changes in both proteins. (*A*) View from a PPHD$_{putida}$ (magenta):EF-Tu (cyan) complex crystal structure reveals EF-Tu in its GDP-bound state; the EF-Tu switch I loop is located in the PPHD active site positioning Pro54 in its *endo*-conformation for *trans*-4-hydroxylation. Six residues (43–48) in the switch I loop are disordered (dotted line). (*Inset*) details of how PPHD interacts with EF-Tu domain II. (*B*) The EF-Tu switch I loop is enclosed in the PPHD catalytic site; the electron density $|F_o - F_c|$ map is in green mesh contoured to 3.0 σ. (*C*) Surface representation of the PPHD$_{putida}$ (magenta):EF-Tu (cyan) complex revealing enclosure of the PPHD$_{putida}$ β2–β3 finger loop and the β5(II)–β6(III) thumb loop around the EF-Tu switch I loop. (*D*) Superimposition of domains II and III of *P. putida* EF-Tu (cyan) in complex with PPHD (rmsd, 0.6 Å; PPHD not shown) and *E. coli* EF-Tu (yellow) (PDB ID: 2BVN) (27) bound to enacyloxin IIA (blue sticks) and a nonhydrolyzable GTP-analog guanosine 5′-(β,γ-imido)triphosphate (GDPNP) (red). (*E*) Superimposition of *E. coli* EF-Tu (PDB ID: 1DG1) (26) and *P. putida* EF-Tu from the PPHD$_{putida}$:EF-Tu complex; the switch I loop is highlighted (*P. putida* EF-Tu, blue; *E. coli* EF-Tu, red). (*F*) Superimposition of the β5(II)–β6(III) thumb loop as in isolated PPHD (green) and in the PPHD$_{putida}$ (magenta):EF-Tu (cyan) complex reveals reorganization of thumb residues on substrate binding: Phe128$_{PPHD}$ rotates 90° to position its phenyl ring directly behind Pro54$_{EF\text{-}Tu}$; Asp131$_{PPHD}$ forms a salt bridge with Arg133$_{PPHD}$; Asp132$_{PPHD}$ rotates 180° to salt bridge to Arg234$_{EF\text{-}Tu}$ of EF-Tu domain II, allowing Arg134$_{PPHD}$ to hydrogen bond to Pro54$_{EF\text{-}Tu}$.

EF-Tu is in its translationally inactive GDP-bound conformational state consistent with the observed PPHD-mediated inhibition of GTP hydrolysis. PPHD$_{putida}$ binds EF-Tu between domain I and domains II/III, occupying a position similar to that observed for EF-Tu domain I in its GTP-bound active state relative to EF-Tu domains II/III (Fig. 3*D*) (27). A Mg(II) ion is present in the EF-Tu nucleotide binding site, as in the EF-Tu structure without PPHD$_{putida}$. Mn(II) and NOG are present in the PPHD$_{putida}$ active site.

In contrast to the isolated EF-Tu$_{putida}$ structure, in the complex, most EF-Tu switch I loop residues are ordered (16 residues disordered in isolated EF-Tu; 6 in the PPHD:EF-Tu complex). In a structure of isolated *E. coli* EF-Tu (in its inactive GDP-bound state), all of the switch I loop residues are ordered and located on the surface of EF-Tu domain I, adopting a loop-helix-loop-strand conformation (Fig. 3*E*) (26). Comparison of the *P. putida* PPHD:EF-Tu complex crystal structure with that of *E. coli* EF-Tu (78% identity; rmsd, 1.2 Å over 338 Cα atoms) reveals major differences. Relative to the isolated *E. coli* EF-Tu structure, in the PPHD:EF-Tu complex structure, the entire EF-Tu switch I loop pivots around residues Gly41$_{EF\text{-}Tu}$ and Ile61$_{EF\text{-}Tu}$, such that Pro54$_{EF\text{-}Tu}$ moves 22 Å and is positioned at the apex of an extended loop projecting into the PPHD$_{putida}$ active site (Fig. 3*E*).

In contrast to the isolated PPHD$_{putida}$ structure, in the PPHD:EF-Tu complex, the PPHD$_{putida}$ β2–β3 finger loop (residues 51–74) is ordered and encloses the EF-Tu switch I loop within the active site (Fig. 3*C*). The residues at the apex of the flexible β2–β3 finger loop of PPHD$_{putida}$ adopt a 3_{10}-helix conformation (residues 58–60). An arginine (Arg57) before the 3_{10}-helix is positioned to form a salt bridge with Asp130 of the β5(II)-β6(III) "thumb" loop (seven residues, 127–133), forming a tunnel through which the EF-Tu switch I loop is threaded (Fig. 3*C*). The β5(II)–β6(III) thumb loop of PPHD$_{putida}$ contains three arginines, three aspartates (including Asp130), and one phenylalanine, the backbone and side chains of which make interactions with domain II of EF-Tu and undergo clear conformational changes relative to their positions in the isolated PPHD$_{putida}$ structure (rmsd, 1.4 Å; Fig. 3*F* and *SI Appendix*, Fig. S6*C*).

As indicated by the kinetic analyses in solution, the PPHD:EF-Tu structure reveals substantial enzyme-substrate contacts beyond the active site. PPHD and EF-Tu share a total interaction interface of 1,662 Å^2 (24 hydrogen bonds; 10 salt bridges), resulting in a calculated $\Delta G_{binding}$ of ~-9.7 kcal/mol, of which only 965 Å^2 (13 hydrogen bonds; 3 salt bridges) is accounted for by direct interactions of PPHD$_{putida}$ with the EF-Tu switch I loop. Other interactions include positioning the PPHD$_{putida}$ α3-helix into a hydrophobic pocket in the β-barrel of EF-Tu domain II formed by Phe222$_{EF\text{-}Tu}$, Ile224$_{EF\text{-}Tu}$, and Val230$_{EF\text{-}Tu}$, and burying Phe265$_{EF\text{-}Tu}$ in a hydrophobic pocket formed by the side chains of Leu101$_{PPHD}$, Leu103$_{PPHD}$, and Leu177$_{PPHD}$ (Fig. 3*A*, *Inset*). These interactions collectively order the PPHD$_{putida}$ thumb loop, suggesting that analogous interactions between PHD2 and full-length HIFα, not observed in a PHD2:HIF-α fragment structure (25), may occur.

Conservation of Substrate Binding by Prolyl-Hydroxylases. The positions of the β2–β3 finger loop residues in the complex are strikingly similar to those observed for PHD2 in complex with HIF-α and to a collagen prolyl-4-hydroxylase-related protein in *Chlamydomonas reinhardtii* (CrP4H) when complexed with a proline-rich substrate (Fig. 4 *A* and *B* and *SI Appendix*, Fig. S6 *D* and *E*) (25, 28). In PHD2 and CrP4H, the β2–β3 finger loop (PHD2: 23 residues, 236–258; CrP4H: 24 residues, 76–99) and β5 (II)–β6(III) thumb loop (PHD2: 6 residues; 316–321; CrP4H: 15 residues, 146–160) are of similar length and in the same locations as those of PPHD$_{putida}$ (Fig. 4 *A* and *B* and *SI Appendix*, Fig. S7 *A* and *B*); however, an analogous Arg57:Asp130 salt bridge that connects the finger and thumb loops is not present in PHD2 or CrP4H.

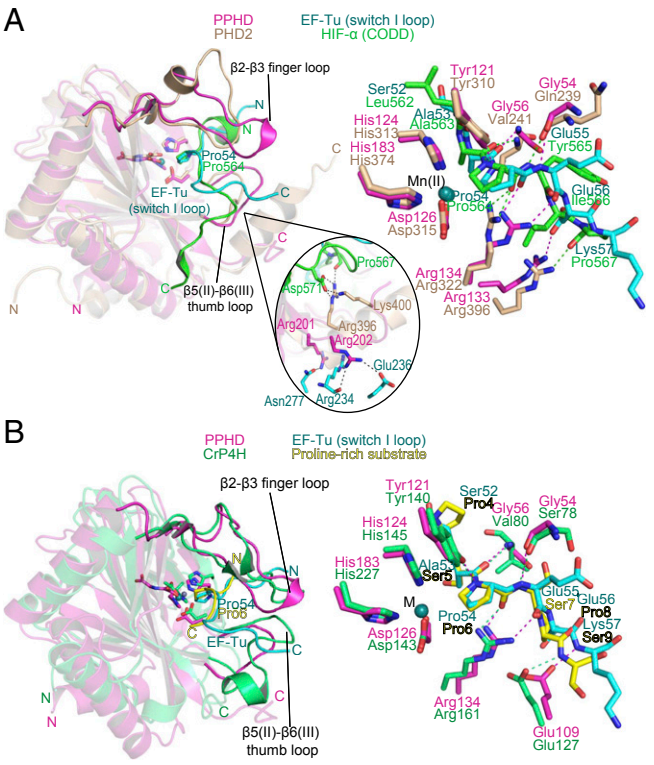

Fig. 4. *Pseudomonas* PPHD, human PHD2, and *C. reinhardtii* P4H (CrP4H) share a conserved mechanism for substrate binding. Overall and active site superimpositions of the PPHD$_{putida}$ (magenta):EF-Tu (cyan) complex and both (*A*) human PHD2 (sand) in complex with HIF-α CODD (residues 556–574; PDB ID: 3HQR) (green) and (*B*) CrP4H (green) in complex with proline-rich peptide substrate (PDB ID: 3GZE) (yellow) reveal conservation of the roles of the β2–β3 finger loop and the β5(II)–β6(III) thumb loop, the orientation of the substrate backbone in the active site, and other key substrate binding interactions. Note that although CrP4H does not share a structurally conserved Arg133$_{PPHD}$ with PPHD, as does PHD2 (*Inset*), CrP4H does share a conserved Glu109$_{PPHD}$ (Glu127$_{CrP4H}$, Thr296$_{PHD2}$). (*Inset*) The PPHD$_{putida}$ and PHD2 *C* termini interact differently with their substrates. In contrast, the PHD2 *C* terminus interacts directly with HIF-α CODD (25).

The PHD2 *C*-terminal α-helix is involved in substrate binding and catalysis (16, 25). The PPHD$_{putida}$ *C*-terminal loop (residues 201–207, corresponding to PHD2 392–408) directly interacts with EF-Tu, as does the PHD2 *C*-terminal α-helix with HIF-α CODD (Fig. 4*A*, *Inset*), suggesting evolutionary conservation of a role for the *C* terminus in substrate recognition.

Comparison of the substrate complexes reveals that conservation is not limited to the enzymes but extends to the bound substrates. Strikingly, the unrelated substrates all adopt closely related conformations in their active site regions when bound to their respective prolyl-hydroxylase partners; EF-Tu (residues 50–57) complexed with PPHD shares a similar orientation and conformation to that of HIF-α (residues 560–567) complexed with PHD2 (backbone atoms rmsd, 0.1 Å) and to that of a proline-rich peptide complexed with CrP4H (backbone atoms rmsd, 0.1 Å; Fig. 4 *A* and *B* and *SI Appendix*, Fig. S6 *D* and *E*). However, there are differences in observed substrate binding for the prolyl-4-hydroxylases (PPHD, PHDs, CP4Hs) and that predicted for prolyl-3-hydroxylases (OGFOD1/Tpa1; *SI Appendix*, Fig. S7 *A* and *B*). The prolyl-4-hydroxylases have a conserved arginine at their active site opening positioned to hydrogen bond to the carbonyl of the substrate proline (Arg134$_{PPHD}$, Arg322$_{PHD2}$, Arg161$_{CrP4H}$). Prolyl-4-hydroxylases also have a conserved tyrosine (Tyr121$_{PPHD}$, Tyr310$_{PHD2}$, Tyr140$_{CrP4H}$), the hydroxyl of which points toward the nitrogen of the substrate proline (Fig. 4 *A* and *B* and *SI Appendix*,

Fig. S6 *D* and *E* and S7*B*). In contrast, the prolyl-3-hydroxylases have a smaller hydrophobic leucine at the equivalent position to $Tyr121_{PPHD}$ ($Leu156_{Tpa1}$, $Leu152_{OGFOD1}$) (29), which may promote prolyl-3-hydroxylation over prolyl-4-hydroxylation by adjusting the position of the proline within the active site.

In the $PPHD_{putida}$ active site, the pyrrolidine ring of $Pro54_{EF\text{-}Tu}$ is observed in a C-4 *endo* conformation, poised for hydroxylation, as observed in the PHD2:HIF-α and CrP4H:proline-rich peptide complexes (Fig. 4 *A* and *B* and *SI Appendix*, Fig. S6 *D* and *E*) (25, 28, 30), and in contrast to the C-4 *exo* conformation, as observed for prolyl-hydroxylated HIF-1α when complexed with pVHL (1).

Discussion

The combined results suggest that roles for prolyl-hydroxylation are ancient, extending from EF-Tu in bacteria to, at least, collagen, HIF-α, and ribosomal protein 23 in eukaryotes. The results support growing evidence for the importance of 2OG oxygenases, including PHD homologs, in the regulation of translation, as well as of transcription (5–8, 29, 31–35). It is notable that the Jumonji C subfamily 2OG oxygenases also play roles in both histone/chromatin and ribosomal protein modification (5, 36).

Structurally guided bioinformatic analyses are informative with regard to the distribution of prolyl-hydroxylases. Comparison of the topologies of the prolyl-3-hydroxylases and prolyl-4-hydroxylases for which crystal structures are available reveals conservation not only of the DSBH, Fe(II), and 2OG binding sites but also of other functionally important elements including the β2–β3 finger loop and α-helices that pack against the DSBH (*SI Appendix*, Fig. S7 *A* and *B*), enabling assignment of putative prolyl-hydroxylases with a high confidence level. All identified subtypes of prolyl-4-hydroxylases (CP4Hs and PHDs) and prolyl-3-hydroxylases [Leprecans (mammalian collagen prolyl-3-hydroxylases) and OGFOD1s] are ubiquitous in animals, and all but the Leprecans are present in choanoflagellates. However, their presence in prokaryotes is sporadic, and they are apparently absent in archaea (Fig. 5 and *SI Appendix*, Fig. S8).

Given that HIF and collagen exist in animals, but not bacteria, protein prolyl-hydroxylases (and other enzymes catalyzing post-translational modifications) may have first evolved to catalyze oxidation of highly abundant proteins, such as the switch I loop of EF-Tu, which are part of the translational machinery. Such protein hydroxylases were possibly derived from 2OG oxygenases acting on small molecules (e.g., proline-hydroxylases) (37), some of which have simpler structures than the protein-hydroxylases (23). In eukaryotes, the prolyl-hydroxylases evolved divergently to catalyze hydroxylation of collagen and other proteins involved in translational and transcriptional regulation [e.g., Skp1 and ribosomal protein 23 (6–9)]. Their role in HIF-α hydroxylation evolved in animals, possibly via fusion of a basic helix–loop–helix domain transcription factor with an EF-Tu, collagen, or Skp1-related or Skp1-derived substrate. The observation that PHD2 interacts with, but apparently does not hydroxylate, eEF2, the eukaryotic counterpart to prokaryotic EF-G, an EF-Tu homolog (15), is interesting because it may reflect an ancestral relationship between PPHD and EF-Tu. Competition between HIF-α and eEF2 [and potentially other PHD substrates; e.g., pyruvate kinase M2 (38) or centrosomal protein 192 (39)], may help regulate the hypoxic response in higher animals. Analogous competition is proposed for factor-inhibiting HIF (FIH) catalyzed HIF-1α asparagine hydroxylation, which reduces HIF activity by blocking its interaction with coactivator proteins (1). Factor-inhibiting HIF also takes ankyrin repeat domains as substrates in a manner proposed to enable a robust and tuneable hypoxic response (40).

The conformational changes observed on substrate binding in the PPHD:EF-Tu complex reveal that major induced fit during 2OG oxygenase catalyzed protein-modification can occur. The observed changes will be useful in designing new types of 2OG oxygenase inhibitors based on various conformational states, rather than active site iron chelators, which make up most reported 2OG oxygenase inhibitors, including PHD inhibitors, in clinical trials (41).

The finding that PPHD regulates the production of pyocyanin implies that iron regulation in *P. aeruginosa* may be important in terms of clinically relevant infections. The role of the PHDs in the hypoxic response has been highlighted in part because of medicinal opportunities relating to the treatment of ischemic and related diseases such as anemia (41). Although regulation of animal PHD activity by iron availability is well-established [cobaltous ion induced erythropoiesis is proposed to be via PHD inhibition (41)], it has had less prominence. *P. aeruginosa* infections, which often occur in hypoxic niches, such as in the cystic fibrosis lung (42), can induce a HIF-mediated hypoxic response in eukaryotic cells by production of small molecule factors, which have been proposed to be cyanide (43). Pyocyanin induces HIF-α up-regulation in human cells (13), likely via PHD inhibition, at least in part by iron sequestration. Thus, it seems that during some infections, prolyl-hydroxylases in both human and bacterial cells may be involved in "cross-talk" involving regulation limited not only by oxygen availability but also by that of iron and, possibly, 2OG (or other tricarboxylic acid cycle intermediate or related compounds) (44). Therefore, the biological roles of the PHDs and PPHDs likely extend beyond hypoxic sensing in an isolated organism.

From a clinical perspective, the work is relevant to ongoing trials involving PHD inhibitors for anemia treatment (41). At least some PHD inhibitors inhibit other 2OG oxygenases (41, 45). There is also increasing use of metal chelators, including orally active compounds (which inhibit the PHDs by iron chelation) (46), for iron overload diseases. Although our work does not predict what effect, if any, application of clinically applied PHD inhibitors/iron chelators will have on the course of infections by bacteria containing PHD homologs, the potential for effects of PHD inhibitors on infection should be considered.

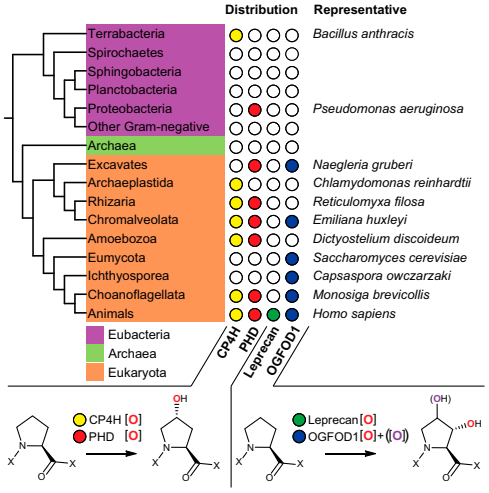

Fig. 5. Distribution of prolyl-hydroxylases in kingdoms of life. Tracking putative homologs of the CP4Hs, PHDs, Leprecans (CP3Hs), and OGFOD1s in representative organisms throughout the kingdoms of life (for phylogenetic analyses encompassing a wider distribution, see *SI Appendix*, Fig. S8). CP4Hs and PHDs catalyze prolyl-4-hydroxylation. Human OGFOD1 catalyzes a single prolyl-3-hydroxylation, whereas its yeast homolog Tpa1 catalyzes a double prolyl-3- and prolyl-4-hydroxylation (7).

Materials and Methods

Protein Purification and Crystallization. Recombinant $PPHD_{putida}$ and $EF\text{-}Tu_{putida}$ were produced in *E. coli* and purified using Ni-affinity and size-exclusion chromatography. For purification of the PPHD:EF-Tu complex, cell pellets containing either $PPHD_{putida}$ or $EF\text{-}Tu_{putida}$ were colysed with Mn(II) and NOG to prevent EF-Tu hydroxylation and were purified in the same way. For details of crystallization conditions, data collection and processing, and refinement statistics, see *SI Appendix, SI Materials and Methods*, and Tables S1 and S2.

***P. aeruginosa* Phenotypic Analyses.** *P. aeruginosa* PAO1 wild-type and PPHD insertional knockout mutant strain were grown (28 °C) in various concentrations of 2,2-bipyridine (0, 1, 5, and 25 mM); the optical density (600 nm, OD_{600}) was assayed every 60 min. For pyocyanin quantification, 5-mL cultures of *P. aeruginosa* wild-type and *PA0310* mutant strains grown to stationary phase were extracted with 3 mL $CHCl_3$ and then back-extracted with 1 mL 0.2 HCl, and then the aqueous phase was decanted and its absorbance measured at 520 nm. For global translation rate assays, 1-mL cultures of *P. aeruginosa* wild-type and *PA0310* mutant strains were grown to log phase (OD_{600} = 0.5), and the rate of incorporation of [^{35}S]methionine (10 μCi/mL) was measured by scintillation counting.

Determination of EF-Tu as a PPHD Substrate. Hydroxylation assays for $PPHD_{putida}$ contained 10 μM PPHD, 100 μM EF-$Tu_{44–63}$ (H_2N-IVEFDKIDSAPEEKARGITI-$CONH_2$), 50 μM Fe(II) [prepared from $(NH_4)_2Fe(SO_4)_2$], 2 mM 2OG, 4 mM sodium L-ascorbate in 50 mM Hepes at pH 7.5, 500 mM NaCl, and 5% (vol/vol) glycerol and were quantified by MALDI MS. MALDI MS/MS was performed to determine the site of hydroxylation. To determine the stereochemistry of hydroxylation, acid hydrolyzed of Hyp54-modified EF-$Tu_{44–63}$ was derivatized and compared with the elution times of hydroxyproline standards. To analyze EF-Tu Pro54 hydroxylation, cells were lysed and analyzed by SDS-PAGE, and the EF-Tu-containing band was excised and subjected to proteosomal digestion (ArgC) and liquid chromatography-MS/MS. For purification of recombinant Hyp54 EF-Tu, $PPHD_{putida}$, Fe(II), 2OG, and sodium L-ascorbic acid were added to the cell lysate at a final concentration of 1 mg/mL, 50 μM, 2 mM, and 4 mM, respectively, and incubated for 1 h at room temperature. The hydroxylation status of Pro54 was then analyzed by trypsinolysis and MSMS analysis.

NMR Experiments. Measurements of Mn(II) and 2OG K_d to $PPHD_{putida}$ used a Bruker AVII 500 instrument. Mixture (160 μL) contained 50 μM apo (i.e. no metal) $PPHD_{putida,}$ 50 μM $MnCl_2$, 50 μM EF-Tu (full length or EF-$Tu_{44–63}$ oligopeptide if required), 10 mM $MgCl_2$ and 200 mM NaCl (buffer: ~30 mM Tris-D11/~20 mM HEPES pH 7.5 in 36.25% H_2O and 63.75% D_2O) (*SI Appendix*, Fig. S6 *F* and *G*). For EF-Tu GTP-GDP turnover assays, we used a Bruker AVIII 700 instrument/5-mm inverse cryoprobe. Incubations (160 μL) contained 10 μM unmodified or Hyp54 EF-Tu, 50 μM kirromycin, 100 μM GTP, 50 μM *apo*-$PPHD_{putida}$ (if required), 100 μM $ZnCl_2$ (if required), 100 μM 2OG (if required), 10 mM $MgCl_2$, and 200 mM NaCl [buffer: 50 mM HEPES (pH 7.5) in 90% H_2O/10% D_2O]. Solutions were buffered using ~30 mM Tris-d11 and ~20 mM Hepes at pH 7.5 in 36.25% H_2O and 63.75% D_2O]. For $ZnCl_2$ inhibition experiments, the mixture contained 10 μM *apo* $PPHD_{putida}$, 50 μM $FeCl_2$, 500 μM 2OG, 600 μM EF-$Tu_{44–63}$, 400 μM $ZnCl_2$ (if required), 1.25 mM ascorbate, and 100 mM NaCl buffered using 50 mM Tris-D11 at pH 7.5 (*SI Appendix*, Fig. S5*D*).

See *SI Appendix, SI Materials and Methods*.

ACKNOWLEDGMENTS. We thank the Diamond Macromolecular Crystallography beamline staff for technical support; Dr. Christoph Loenarz and Prof. Peter J. Ratcliffe for helpful discussion; and the Rhodes Trust (J.S.S.), the British Heart Foundation (I.K.H.L.), the Wellcome Trust, the European Research Council, the Japan Society for the Promotion of Science (S.H.), and the Biotechnology and Biological Sciences Research Council for financial support.

1. Kaelin WG, Jr, Ratcliffe PJ (2008) Oxygen sensing by metazoans: The central role of the HIF hydroxylase pathway. *Mol Cell* 30(4):393–402.
2. Semenza GL (2011) Oxygen sensing, homeostasis, and disease. *N Engl J Med* 365(6): 537–547.
3. Loenarz C, et al. (2011) The hypoxia-inducible transcription factor pathway regulates oxygen sensing in the simplest animal, Trichoplax adhaerens. *EMBO Rep* 12(1):63–70.
4. Myllyharju J, Kivirikko KI (2004) Collagens, modifying enzymes and their mutations in humans, flies and worms. *Trends Genet* 20(1):33–43.
5. Ge W, et al. (2012) Oxygenase-catalyzed ribosome hydroxylation occurs in prokaryotes and humans. *Nat Chem Biol* 8(12):960–962.
6. Singleton RS, et al. (2014) OGFOD1 catalyzes prolyl hydroxylation of RPS23 and is involved in translation control and stress granule formation. *Proc Natl Acad Sci USA* 111(11):4031–4036.
7. Loenarz C, et al. (2014) Hydroxylation of the eukaryotic ribosomal decoding center affects translational accuracy. *Proc Natl Acad Sci USA* 111(11):4019–4024.
8. Katz MJ, et al. (2014) Sudestada1, a Drosophila ribosomal prolyl-hydroxylase required for mRNA translation, cell homeostasis, and organ growth. *Proc Natl Acad Sci USA* 111(11):4025–4030.
9. van der Wel H, Ercan A, West CM (2005) The Skp1 prolyl hydroxylase from Dictyostelium is related to the hypoxia-inducible factor-alpha class of animal prolyl 4-hydroxylases. *J Biol Chem* 280(15):14645–14655.
10. McDonough MA, et al. (2006) Cellular oxygen sensing: Crystal structure of hypoxia-inducible factor prolyl hydroxylase (PHD2). *Proc Natl Acad Sci USA* 103(26):9814–9819.
11. Aravind L, Koonin EV (2001) The DNA-repair protein AlkB, EGL-9, and leprecan define new families of 2-oxoglutarate- and iron-dependent dioxygenases. *Genome Biol* 2(3): RESEARCH0007.
12. Lau GW, Hassett DJ, Ran H, Kong F (2004) The role of pyocyanin in Pseudomonas aeruginosa infection. *Trends Mol Med* 10(12):599–606.
13. Ahmad IM, Britigan BE, Abdalla MY (2011) Oxidation of thiols and modification of redox-sensitive signaling in human lung epithelial cells exposed to Pseudomonas pyocyanin. *J Toxicol Environ Health A* 74(1):43–51.
14. Gupta N, et al. (2007) Whole proteome analysis of post-translational modifications: Applications of mass-spectrometry for proteogenomic annotation. *Genome Res* 17(9): 1362–1377.
15. Romero-Ruiz A, et al. (2012) Prolyl hydroxylase-dependent modulation of eukaryotic elongation factor 2 activity and protein translation under acute hypoxia. *J Biol Chem* 287(12):9651–9658.
16. Flashman E, et al. (2008) Kinetic rationale for selectivity toward N- and C-terminal oxygen-dependent degradation domain substrates mediated by a loop region of hypoxia-inducible factor prolyl hydroxylases. *J Biol Chem* 283(7):3808–3815.
17. Ehrismann D, et al. (2007) Studies on the activity of the hypoxia-inducible-factor hydroxylases using an oxygen consumption assay. *Biochem J* 401(1):227–234.
18. McNeill LA, et al. (2005) Hypoxia-inducible factor prolyl hydroxylase 2 has a high affinity for ferrous iron and 2-oxoglutarate. *Mol Biosyst* 1(4):321–324.
19. Hirsilä M, Koivunen P, Günzler V, Kivirikko KI, Myllyharju J (2003) Characterization of the human prolyl 4-hydroxylases that modify the hypoxia-inducible factor. *J Biol Chem* 278(33):30772–30780.
20. Flashman E, Davies SL, Yeoh KK, Schofield CJ (2010) Investigating the dependence of the hypoxia-inducible factor hydroxylases (factor inhibiting HIF and prolyl hydroxylase domain 2) on ascorbate and other reducing agents. *Biochem J* 427(1):135–142.
21. Voorhees RM, Schmeing TM, Kelley AC, Ramakrishnan V (2010) The mechanism for activation of GTP hydrolysis on the ribosome. *Science* 330(6005):835–838.
22. Villa E, et al. (2009) Ribosome-induced changes in elongation factor Tu conformation control GTP hydrolysis. *Proc Natl Acad Sci USA* 106(4):1063–1068.
23. Clifton IJ, et al. (2006) Structural studies on 2-oxoglutarate oxygenases and related double-stranded beta-helix fold proteins. *J Inorg Biochem* 100(4):644–669.
24. Aik W, McDonough MA, Thalhammer A, Chowdhury R, Schofield CJ (2012) Role of the jelly-roll fold in substrate binding by 2-oxoglutarate oxygenases. *Curr Opin Struct Biol* 22(6):691–700.
25. Chowdhury R, et al. (2009) Structural basis for binding of hypoxia-inducible factor to the oxygen-sensing prolyl hydroxylases. *Structure* 17(7):981–989.
26. Abel K, Yoder MD, Hilgenfeld R, Jurnak F (1996) An alpha to beta conformational switch in EF-Tu. *Structure* 4(10):1153–1159.
27. Parmeggiani A, et al. (2006) Enacyloxin IIa pinpoints a binding pocket of elongation factor Tu for development of novel antibiotics. *J Biol Chem* 281(5):2893–2900.
28. Koski MK, et al. (2009) The crystal structure of an algal prolyl 4-hydroxylase complexed with a proline-rich peptide reveals a novel buried tripeptide binding motif. *J Biol Chem* 284(37):25290–25301.
29. Kim HS, et al. (2010) Crystal structure of Tpa1 from Saccharomyces cerevisiae, a component of the messenger ribonucleoprotein complex. *Nucleic Acids Res* 38(6):2099–2110.
30. Loenarz C, et al. (2009) Evidence for a stereoelectronic effect in human oxygen sensing. *Angew Chem Int Ed Engl* 48(10):1784–1787.
31. Jia G, Fu Y, He C (2013) Reversible RNA adenosine methylation in biological regulation. *Trends Genet* 29(2):108–115.
32. Feng T, et al. (2014) Optimal translational termination requires C4 lysyl hydroxylation of eRF1. *Mol Cell* 53(4):645–654.
33. Henri J, et al. (2010) Structural and functional insights into Saccharomyces cerevisiae Tpa1, a putative prolylhydroxylase influencing translation termination and transcription. *J Biol Chem* 285(40):30767–30778.
34. Lee CY, Yeh TL, Hughes BT, Espenshade PJ (2011) Regulation of the Sre1 hypoxic transcription factor by oxygen-dependent control of DNA binding. *Mol Cell* 44(2): 225–234.
35. van den Born E, et al. (2011) ALKBH8-mediated formation of a novel diastereomeric pair of wobble nucleosides in mammalian tRNA. *Nat Commun* 2:172.
36. Klose RJ, Zhang Y (2007) Regulation of histone methylation by demethylimination and demethylation. *Nat Rev Mol Cell Biol* 8(4):307–318.
37. Hausinger RP (2004) FeII/alpha-ketoglutarate-dependent hydroxylases and related enzymes. *Crit Rev Biochem Mol Biol* 39(1):21–68.
38. Luo W, et al. (2011) Pyruvate kinase M2 is a PHD3-stimulated coactivator for hypoxia-inducible factor 1. *Cell* 145(5):732–744.
39. Moser SC, et al. (2013) PHD1 links cell-cycle progression to oxygen sensing through hydroxylation of the centrosomal protein Cep192. *Dev Cell* 26(4):381–392.
40. Cockman ME, et al. (2006) Posttranslational hydroxylation of ankyrin repeats in IkappaB proteins by the hypoxia-inducible factor (HIF) asparaginyl hydroxylase, factor inhibiting HIF (FIH). *Proc Natl Acad Sci USA* 103(40):14767–14772.
41. Rose NR, McDonough MA, King ON, Kawamura A, Schofield CJ (2011) Inhibition of 2-oxoglutarate dependent oxygenases. *Chem Soc Rev* 40(8):4364–4397.
42. Schaible B, Schaffer K, Taylor CT (2010) Hypoxia, innate immunity and infection in the lung. *Respir Physiol Neurobiol* 174(3):235–243.
43. Budde MW, Roth MB (2011) The response of Caenorhabditis elegans to hydrogen sulfide and hydrogen cyanide. *Genetics* 189(2):521–532.
44. Frezza C, Pollard PJ, Gottlieb E (2011) Inborn and acquired metabolic defects in cancer. *J Mol Med (Berl)* 89(3):213–220.
45. Aik W, et al. (2013) Structural basis for inhibition of the fat mass and obesity associated protein (FTO). *J Med Chem* 56(9):3680–3688.
46. Cho EA, et al. (2013) Differential in vitro and cellular effects of iron chelators for hypoxia inducible factor hydroxylases. *J Cell Biochem* 114(4):864–873.